

## SOLAR NEUTRON EVENTS OF 2003 OCTOBER–NOVEMBER

K. WATANABE,<sup>1</sup> M. GROS,<sup>2</sup> P. H. STOKER,<sup>3</sup> K. KUDELA,<sup>4</sup> C. LOPATE,<sup>5</sup> J. F. VALDÉS-GALICIA,<sup>6</sup> A. HURTADO,<sup>6</sup>  
O. MUSALEM,<sup>6</sup> R. OGASAWARA,<sup>7</sup> Y. MIZUMOTO,<sup>7</sup> M. NAKAGIRI,<sup>7</sup> A. MIYASHITA,<sup>8</sup> Y. MATSUBARA,<sup>1</sup>  
T. SAKO,<sup>1</sup> Y. MURAKI,<sup>1</sup> T. SAKAI,<sup>9</sup> AND S. SHIBATA<sup>10</sup>

Received 2005 July 9; accepted 2005 September 14

### ABSTRACT

During the period when the Sun was intensely active in 2003 October–November, two remarkable solar neutron events were observed by the ground-based neutron monitors. On 2003 October 28, in association with an X17.2 large flare, solar neutrons were detected with high statistical significance ( $6.4 \sigma$ ) by the neutron monitor at Tsumeb, Namibia. On 2003 November 4, in association with an X28-class flare, relativistic solar neutrons were observed by the neutron monitors at Haleakala in Hawaii and Mexico City and by the solar neutron telescope at Mauna Kea in Hawaii simultaneously. Clear excesses were observed at the same time by these detectors, with the significance calculated as  $7.5 \sigma$  for Haleakala and  $5.2 \sigma$  for Mexico City. The detector on board the *INTEGRAL* satellite observed a high flux of hard X-rays and  $\gamma$ -rays at the same time in these events. By using the time profiles of the  $\gamma$ -ray lines, we can explain the time profile of the neutron monitor. It appears that neutrons were produced at the same time as the  $\gamma$ -ray emission.

*Subject headings:* acceleration of particles — cosmic rays — radiation mechanisms: nonthermal — Sun: flares — Sun: particle emission — Sun: X-rays, gamma rays

### 1. INTRODUCTION

Relativistic particles, in particular solar neutrons, give information about ion acceleration in solar flares. Several observations of solar neutrons in solar cycle 23 have been reported using the international network of neutron monitors (Usoskin et al. 1997; Lockwood & Debrunner 1999) and solar neutron telescopes (Tsuchiya et al. 2001; Valdés-Galicia et al. 2004). Solar flares that produce neutrons frequently occur when activity is near its maximum during a solar cycle. In most cases they have also produced X-class solar flares. More than 100 X-class flares have been recorded in this solar cycle.

Intense solar activity occurred from 2003 late October to the beginning of November. The events that occurred in this period were observed by numerous satellites and detectors and have been analyzed by many investigators. During the period when three active regions appeared simultaneously on the Sun, the soft X-ray flux was very intense and a series of 11 X-class solar flares occurred in NOAA regions 10484, 10486, and 10488. At this time, solar neutrons were observed on 2003 October 28 and

November 4, in association with X17.2- and X28-class solar flares, respectively.

The X17.2 solar flare on 2003 October 28 was a remarkable event in this solar cycle. Not only was this a large event, but many phenomena were observed in association with this flare. It is particularly worth noting the large flux of relativistic particles at the Earth (Veselovsky et al. 2004; Panasyuk et al. 2004). Among these particles were solar neutrons that were observed by the ground-based neutron monitor before the main ground-level enhancement (GLE). This solar neutron event has already been reported and discussed by Bieber et al. (2005). In this paper, we compare neutron data with  $\gamma$ -ray data observed by the *International Gamma-Ray Astrophysics Laboratory (INTEGRAL)* satellite and derive the energy spectrum of neutrons using these  $\gamma$ -ray data.

The second event occurred on 2003 November 4, and solar neutrons were observed by NM64-type neutron monitors located at different places, one at Haleakala in Hawaii and the other in Mexico City in Mexico. In addition, solar neutrons were also observed by a solar neutron telescope located at Mauna Kea in Hawaii. Thus, it is important for a single model to be able to explain the data of the three detectors to lead to an accurate spectrum of solar neutrons from the solar neutron event.

Simultaneous observations of solar neutrons have been made for a few events. In the solar event of 1982 June 3, neutrons were simultaneously observed by a ground-level detector and by spacecraft (Chupp et al. 1987). High-energy neutrons were detected by the IGY type neutron monitor installed at Jungfraujoch, Switzerland, and low-energy neutrons and high-energy  $\gamma$ -rays were observed by the Gamma Ray Spectrometer (GRS) on board the *Solar Maximum Mission (SMM)*.

On 1990 May 24, solar neutrons were simultaneously observed by the IGY type neutron monitors located at Climax and several stations in North America (Shea et al. 1991; Debrunner et al. 1997; Muraki & Shibata 1996). On 1991 June 4, solar neutron signals were recorded by the neutron monitor and the solar neutron telescope located at Mount Norikura (Muraki et al. 1992; Struminsky et al. 1994). However, in this event, the energy spectrum of solar neutrons calculated from the data of these detectors was not

<sup>1</sup> Solar-Terrestrial Environment Laboratory, Nagoya University, Furo-cho, Chikusa-ku, Nagoya 464-8601, Japan.

<sup>2</sup> Direction des Sciences de la Matière/DAPNIA/SAP, Commissariat à l’Energie Atomique, Saclay, 91191 Gif-sur-Yvette, France.

<sup>3</sup> Potchefstroom Campus, North-West University, Private Bag X6001, Potchefstroom 2520, South Africa.

<sup>4</sup> Institute of Experimental Physics SAS, Watsonova, 47 040 01 Kosice, Slovakia.

<sup>5</sup> University of New Hampshire, Space Science Center, Morse Hall, 39 College Road, Durham, NH 03824.

<sup>6</sup> Instituto de Geofísica, Universidad Nacional Autónoma de México, Ciudad Universitaria, Del Coyoacán México, C. P. 04510, D. F. México, Mexico.

<sup>7</sup> National Astronomical Observatory of Japan, Osawa, Mitaka, Tokyo 181-8588, Japan.

<sup>8</sup> Subaru Telescope, National Astronomical Observatory of Japan, 650 North A’ohoku Place, Hilo, HI 96720.

<sup>9</sup> College of Industrial Technologies, Nihon University, 2-11-1, Shinei, Narashino, Chiba 275-0005, Japan.

<sup>10</sup> College of Engineering, Chubu University, Kasugai, Aichi 487-8501, Japan.

self-consistent. This discrepancy came from the propagation model of solar neutrons in the Earth's atmosphere. By using the same propagation model, which is the Shibata model (Shibata 1994), nearly the same spectrum was obtained (Shibata et al. 1993). In this paper, we report the analysis results of the November 4 event using data from the neutron monitors, the solar neutron telescope, and the spacecraft. Our model can explain data from the three detectors consistently.

## 2. SOLAR NEUTRON EVENT ASSOCIATED WITH AN X17.2 FLARE ON 2003 OCTOBER 28

### 2.1. Observations

An X17.2-class solar flare occurred at 9:51 UT (time observed at Earth; same definition is used hereafter) on 2003 October 28 located in NOAA active region 10486 at S16°, E08°. From 10:36 to 11:06 UT, an interval that includes the start time of intense emission of soft X-rays from the X17.2 flare, the *RHESSI* (*Reuven Ramaty High Energy Solar Spectroscopic Imager*) satellite was, unfortunately, in the South Atlantic Anomaly (SAA). However, intense emission of high-energy  $\gamma$ -rays was seen in the data after 11:06 UT, indicating that strong particle acceleration occurred during this flare.

On the other hand, large fluxes of hard X-rays and  $\gamma$ -rays were observed by the *INTEGRAL* satellite shortly after 11:00 UT. Figure 1 shows the bremsstrahlung and line  $\gamma$ -ray time profiles from *INTEGRAL*. In the top panel of Figure 1, two peaks of intense emission of bremsstrahlung  $\gamma$ -rays are seen at around 11:03 and 11:05 UT. However, there is only one peak (around 11:05 UT) in line  $\gamma$ -ray time profiles as shown in the second to fourth panels in Figure 1. This more or less coincides with the second peak in the bremsstrahlung  $\gamma$ -rays.

Figure 2 shows  $\gamma$ -ray spectra between 11:02 and 11:03 UT and between 11:03 and 11:15 UT. From 11:02 to 11:03 UT, when the first peak of bremsstrahlung  $\gamma$ -rays was seen, there is no line  $\gamma$ -ray component. The  $\gamma$ -ray lines were clearly seen in the  $\gamma$ -ray spectrum after 11:03 UT, consistent with the line  $\gamma$ -ray time profiles shown in Figure 1. Thus, it appears that the time profiles of ion and electron acceleration were quite different at this event, and ion acceleration either did not occur or was quite weak during the first peak of the bremsstrahlung  $\gamma$ -rays. We can assume that the ion acceleration started only after 11:03 UT.

In Figure 1, note that the 2.2 MeV neutron capture  $\gamma$ -ray line peaks around 11:06 UT and has a long decay time. The 4.4 and 6.1 MeV  $\gamma$ -ray lines of de-excited C and O ions peak around 11:05 UT, giving about a 1 minute gap between the two peak times. In general, neutron capture  $\gamma$ -rays are delayed from  $\gamma$ -ray lines of de-excited ions, since it takes time for high-energy neutrons to slow down and be captured by protons (Wang & Ramaty 1974). Thus, it is evident that solar neutrons were produced at this flare, and they were probably produced at the same time that 4.4 and 6.1 MeV  $\gamma$ -ray lines were emitted. Hereafter, we assume that solar neutrons were produced around 11:05 UT.

At 11:05 UT on 2003 October 28, the Sun was located over Africa. Among our international network of solar neutron telescopes, Gornergrat in Switzerland and Aragats in Armenia had a possibility of observing solar neutrons. On the other hand, Tsumeb observatory (17°6E, 19°1S; 1240 m above sea level [a.s.l.]) was located just under the Sun at this time. The altitude of Tsumeb Observatory is a little bit low; however, the air mass for the line of sight to the Sun was thinner than that of any other observatory because the zenith angle of the Sun was 9°5'. Solar neutrons were clearly observed by the Tsumeb neutron monitor (Bieber et al. 2005).

The 5 minute counting rate of the Tsumeb neutron monitor is shown in Figure 3 (*top*). Clear excesses are seen between 11:05 and 11:15 UT and between 11:20 and 11:25 UT. The statistical significances of these excesses are 4.8  $\sigma$  for 11:05–11:10 UT, 4.2  $\sigma$  for 11:10–11:15 UT, and 3.4  $\sigma$  for 11:20–11:25 UT. The total significance for the 10 minutes between 11:05 and 11:15 UT is 6.4  $\sigma$ .

At the same time, high-energy protons were produced in association with this flare, and large ground-level enhancements (GLEs) occurred around the world. We can exclude the possibility that excesses observed at Tsumeb came from energetic ions by considering the time profile of the neutron monitor at Lomnicky Stit (20°2E, 49°2N; 2634 m a.s.l.), together with that of Tsumeb's neutron monitor (Fig. 3, *bottom*). The start time of the first excess of the Tsumeb neutron monitor is about 10 minutes earlier than the event at Lomnicky Stit, while the second excess at Tsumeb is consistent with this event at Lomnicky Stit. Thus, it appears that the second excess at Tsumeb came from energetic ions and the first excess was solar neutrons.

### 2.2. Analysis Result

Using observational data presented in § 2.1, we can calculate the energy spectrum of the solar neutrons even though neutron monitors cannot measure the energy of neutrons. By using the time of flight (TOF) method and assuming the emission time of solar neutrons, a spectrum can be derived. We assume that the neutrons were produced at 11:05 UT, when line  $\gamma$ -ray emission peaked, and that the energy of the neutrons responsible for the excesses recorded by the neutron monitor is greater than 100 MeV.

From the time profile of the neutrons, we calculate the energy spectrum of solar neutrons at the solar surface by the following formula:

$$\frac{\Delta N}{\epsilon S \Delta E_n P}, \quad (1)$$

where  $\Delta N$  is the number of excess counts contributed by solar neutrons and  $\epsilon$  is the detection efficiency of the neutron monitor. Here  $\epsilon$  includes the attenuation of solar neutrons through the Earth's atmosphere;  $S$  is the area of the neutron monitor,  $\Delta E_n$  is the energy range corresponding to one time bin, and  $P$  is the survival probability of solar neutrons traveling from the Sun to the Earth.

To obtain the  $\epsilon$  of equation (1), we calculated the attenuation of solar neutrons by the Earth's atmosphere using the Shibata model (Shibata 1994). Solar neutrons with energy less than 100 MeV are strongly attenuated by the Earth's atmosphere, so the detection of neutrons by the Tsumeb monitor directly implies that the spectrum extended beyond 100 MeV. For the detection efficiency of the neutron monitor, we used the result calculated by Clem & Dorman (2000).

Using these observational and simulation results, we calculated the energy spectrum of neutrons at the solar surface using the method used for the solar neutron event observed on 2000 November 24 (Watanabe et al. 2003). Figure 4 shows the result from equation (1). By fitting these data points with a power law of the form  $C(E_n/100 \text{ MeV})^\alpha$ , the energy spectrum of solar neutrons was obtained. The energy spectrum is fitted by a power law as

$$(3.1 \pm 1.0) \times 10^{27} \left( \frac{E_n}{100 \text{ MeV}} \right)^{-3.6 \pm 0.3} \text{ MeV}^{-1} \text{ sr}^{-1}. \quad (2)$$

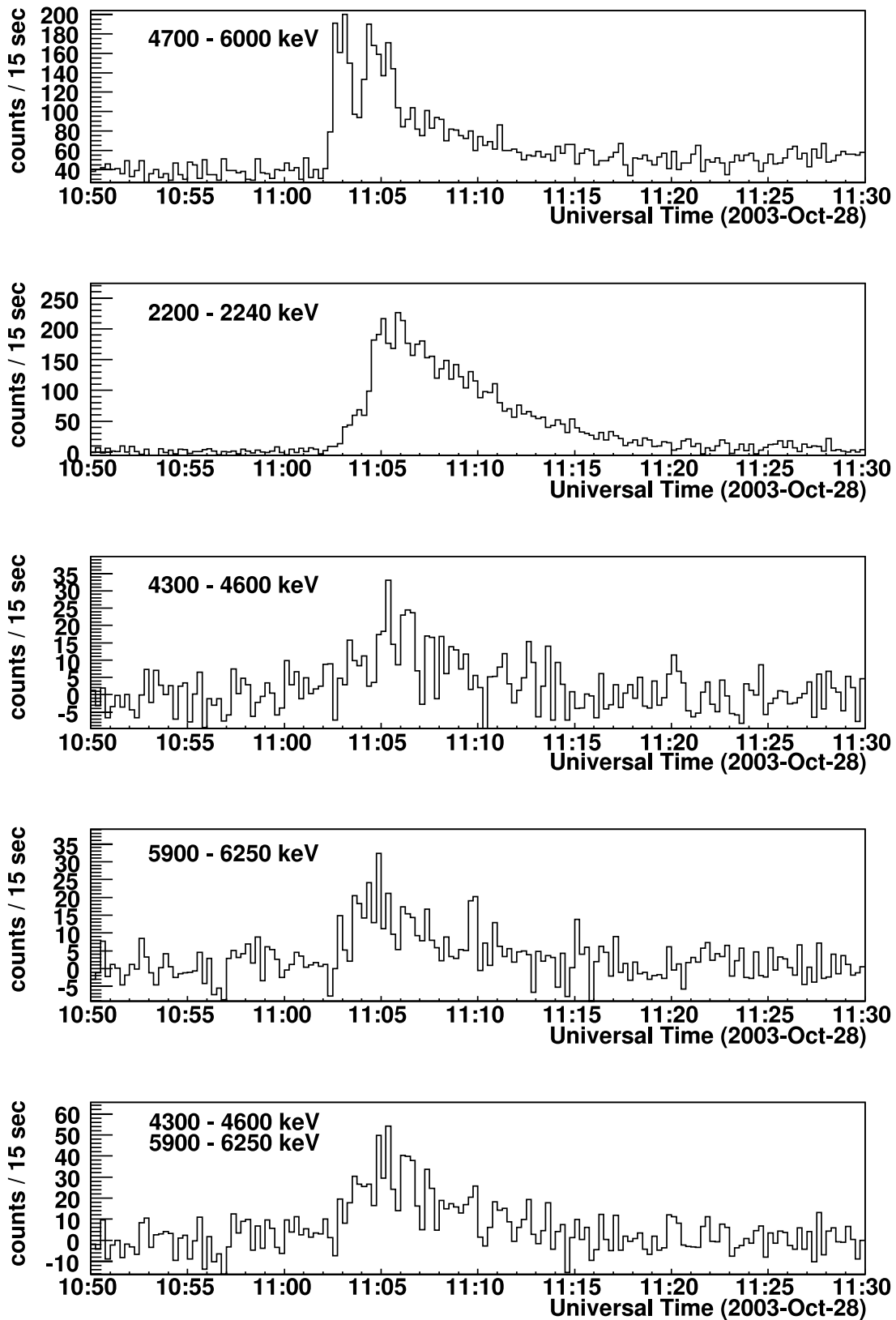


FIG. 1.—*Top panel:* Time profile of bremsstrahlung  $\gamma$ -rays observed by the *INTEGRAL* satellite on 2003 October 28. *Second to fourth panels:* Line  $\gamma$ -ray time profiles observed by the *INTEGRAL* satellite on 2003 October 28. The bremsstrahlung component has been subtracted. *Second panel:* Time profile of the 2.2 MeV neutron capture  $\gamma$ -rays. *Third panel:* Profile of 4.4 MeV  $\gamma$ -rays of C nuclei. *Fourth panel:* Profile of 6.1 MeV  $\gamma$ -rays of O nuclei. *Bottom panel:* Sum of the data in the third and fourth panels.

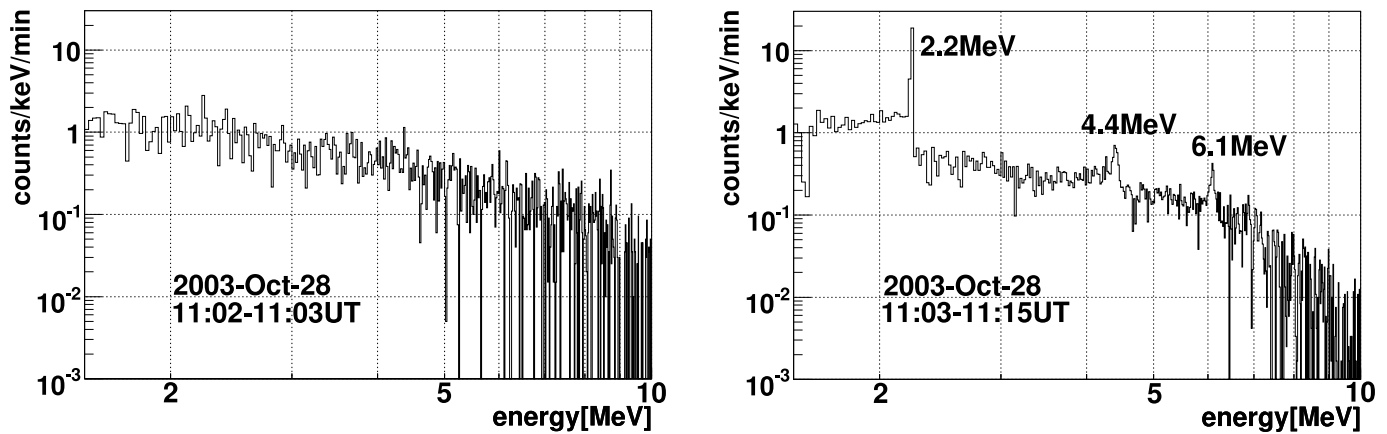


FIG. 2.—Spectra of  $\gamma$ -rays between 1.5 and 10 MeV observed by *INTEGRAL* at 11:02–11:03 UT (*left*) and 11:03–11:15 UT (*right*) on 2003 October 28, with background subtracted. *Right*: Clear signals of 2.2, 4.4, and 6.1 MeV  $\gamma$ -rays appear superimposed on the bremsstrahlung component.

For this fit,  $\chi^2/\text{dof} = 7.10/8 = 0.89$ , and the  $\chi^2$  probability is 53%. The fitting region is above 100 MeV. This power index is a typical value for solar neutron events observed thus far. The total energy flux of  $>100$  MeV neutrons emitted by the Sun was estimated to be  $3.1 \times 10^{25}$  ergs  $\text{sr}^{-1}$ .

### 2.2.1. Simulation by Impulsive Model

In the analysis method described above, the energy spectrum is calculated by dividing the response into several bins, each characterized by a mean energy. For the survival probability of solar neutrons, as well as the attenuation of neutrons and detection efficiency of the neutron monitor, the values at these discrete energies are used. In order to calculate the energy spectrum of the solar neutrons in detail, we include an assumption about the time profiles of solar neutrons but still assume a power-law spectral index at the solar surface. Using this method, we can investigate whether the neutrons are produced continuously. To clarify the consistency with the conventional method, we begin by assuming that the neutrons are produced impulsively.

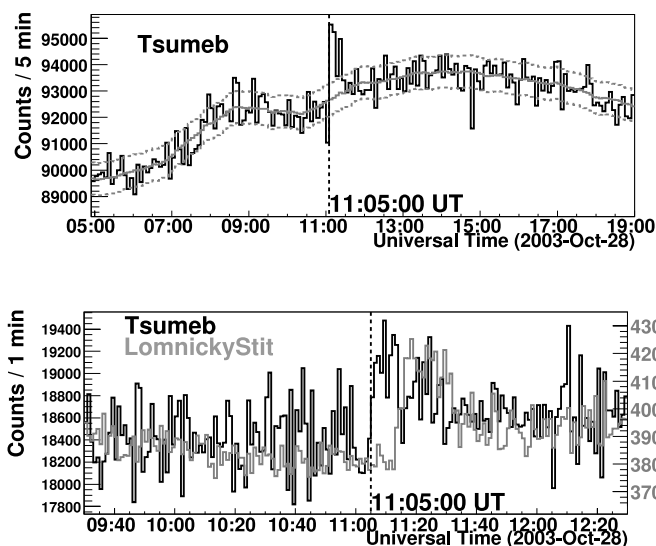


FIG. 3.—*Top*: 5 minute counting rate observed by the Tsumeb neutron monitor on 2003 October 28. The smooth solid line is the averaged background, and the dashed lines are  $\pm 1\sigma$  from the background. *Bottom*: 1 minute counting rate of the Tsumeb neutron monitor (*black line*) and time profile of the Lomnický Stit neutron monitor (*gray line*). The solar neutron event in the Tsumeb data started well before the GLE event seen at Lomnický Stit.

In this simulation, the power index of the neutron spectrum at the Sun is changed from  $-1.5$  to  $-7.0$  with a step of  $0.1$ , while the energy range of the incident neutrons is confined to  $50$ – $1500$  MeV. The time profile of neutrons detected by the neutron monitor is calculated using the neutron attenuation in the Earth's atmosphere given by the Shibata model (Shibata 1994) and the detection efficiency of the neutron monitor as calculated by Clem & Dorman (2000). The decay of neutrons between the Sun and the Earth is also taken into account. The result of this simulation can then be compared with the observational data, normalizing the simulated counting rate ( $N$ ) to the observed excess counting rate ( $N_0$ ).

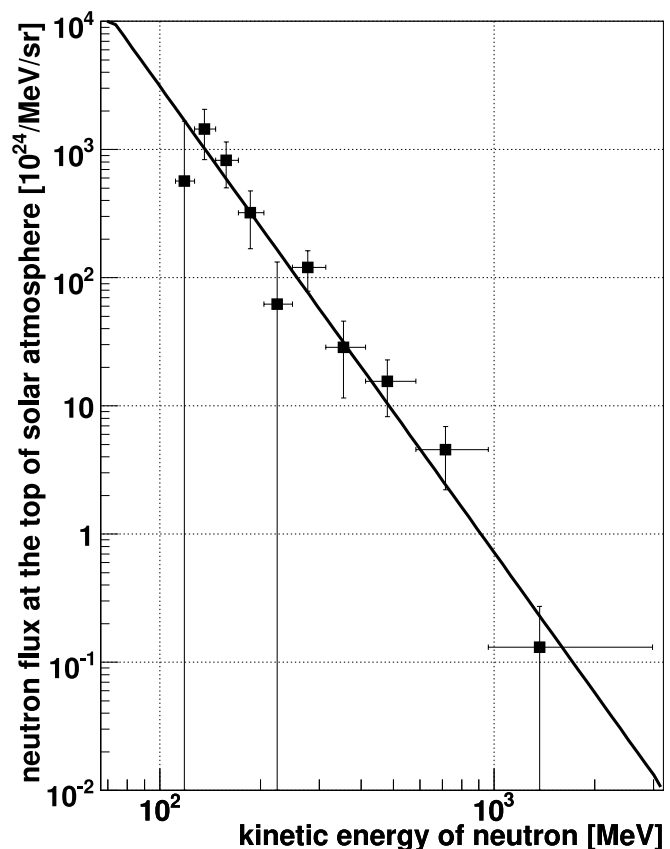


FIG. 4.—Energy spectrum of neutrons at the solar surface on 2003 October 28.

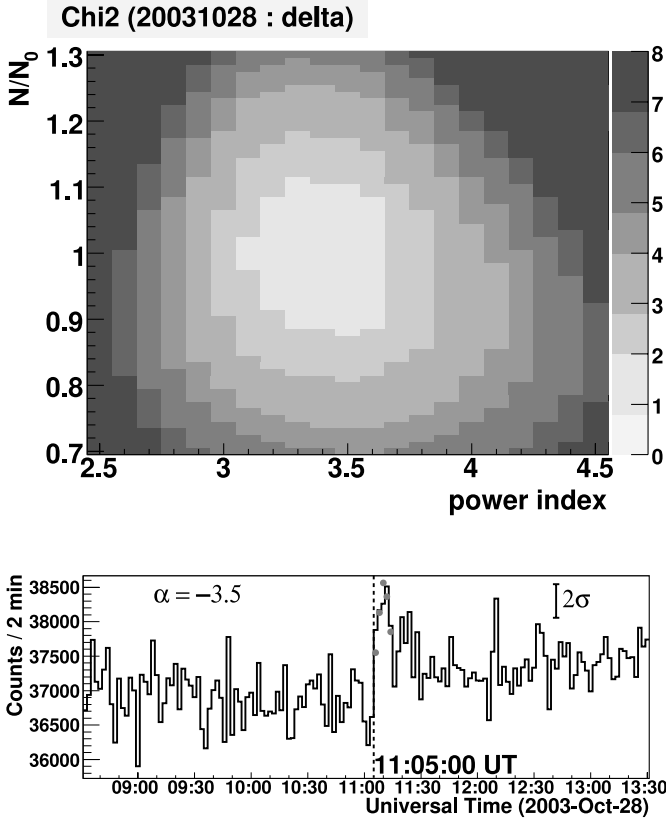


FIG. 5.—*Top*: Reduced  $\chi^2$ -distribution of the fit of the simulated counting rate to the observed excess of the Tsumeb neutron monitor. A 2 minute counting rate is used in this calculation. The  $x$ -axis represents the power index of the simulated time profiles, and the  $y$ -axis corresponds to the ratio of the simulated counting rate ( $N$ ) to the observed one ( $N_0$ ). In this fitting, data obtained during 11:05–11:15 UT are used. *Bottom*: 2 minute counting rate (solid line) observed by the Tsumeb neutron monitor on 2003 October 28, together with simulated time profile (points) for which solar neutrons are assumed to be produced instantaneously at 11:05 UT, when power index is  $-3.5$ .

Figure 5 (*top*) shows the reduced  $\chi^2$ -distribution of the fit of the simulated counting rate to the observed excess of the Tsumeb neutron monitor obtained from the following formula:

$$\chi^2 = \sum_{i=1}^n \frac{(N_i - N_{0i})^2}{N_{0i}}. \quad (3)$$

In this fitting, data obtained from 11:05 to 11:15 UT are used. The  $\chi^2$  has its smallest value when the spectral index is around  $-3.5$ . When the spectral index is  $-3.5$ , the simulated result reproduces the observed result as shown in Figure 5 (*bottom*), where  $\chi^2/\text{dof} = 6.07/4 = 1.52$ , which yields the minimum  $\chi^2$  for the simulated time profile. From this fitting, the energy spectrum is determined as follows:

$$(3.3 \pm 0.3) \times 10^{27} \left( \frac{E_n}{100 \text{ MeV}} \right)^{-3.5^{+0.4}_{-0.2}} \text{ MeV}^{-1} \text{ sr}^{-1}. \quad (4)$$

This is comparable to the result obtained using the simpler method shown in equation (2), but the total energy flux of solar neutrons with energy range between 50 and 1500 MeV is  $9.8^{+1.2}_{-0.9} \times 10^{25} \text{ ergs sr}^{-1}$ , about a factor of 3 higher than the other estimate. This is because of the lower cutoff energy of the neutron spectra.

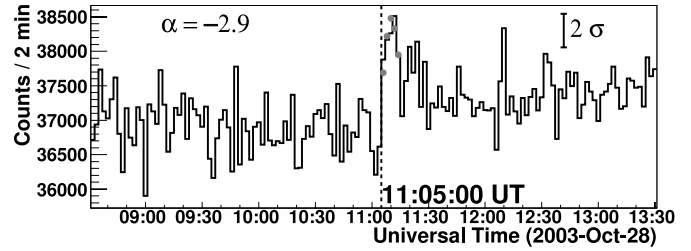


FIG. 6.—Observed and simulated time profiles of the Tsumeb neutron monitor. The solid line is the observed 2 minute counting rate, and points indicate the best-fit simulated time profile for solar neutrons assumed to be produced with the same time profile as  $\gamma$ -ray lines.

### 2.2.2. Simulation by Neutron Production with $\gamma$ -Ray Time Profile

We next simulated the neutron time profiles detected at Tsumeb by assuming that neutrons were produced with a time spread, since extended production of line  $\gamma$ -rays was observed by *INTEGRAL*. For this calculation, we used the summed time profile of 4.4 and 6.1 MeV  $\gamma$ -rays as shown in the bottom panel of Figure 1 as the production model of solar neutrons. These are the  $\gamma$ -ray lines of carbon and oxygen, which indicate the time profile of ion acceleration. We used the data observed from 11:02:45 to 11:10:00 UT. The spectral index of neutrons at the Sun is varied from  $-1.1$  to  $-7.0$  in steps of 0.1. The energy range of the neutrons is again taken to be 50–1500 MeV.

The  $\chi^2$  for the fit were calculated by using data obtained from 11:05 to 11:15 UT. The  $\chi^2$  has its smallest value for the spectral index  $-2.9$ . The simulated result reproduces the observed result most closely when the spectral index is  $-2.9$  as shown in Figure 6. When the spectral index is  $-2.9$ ,  $\chi^2/\text{dof} = 2.76/4 = 0.69$ , which provides the minimum  $\chi^2$  for the simulated time profiles. From this fit, the spectral index is found to be  $-2.9 \pm 0.3$ . The best-fit spectral index is harder than the index derived on the assumption that the neutrons were produced impulsively, but the total energy flux of the neutrons is now estimated to be  $6.2^{+0.5}_{-0.6} \times 10^{25} \text{ ergs sr}^{-1}$ , not very much different from the result for impulsive production.

## 3. SIMULTANEOUS OBSERVATIONS OF SOLAR NEUTRONS ON 2003 NOVEMBER 4

### 3.1. Observations

On 2003 November 4, an X28-class solar flare occurred at 19:29 UT, located in NOAA active region 10486 at  $S19^\circ$ ,  $W83^\circ$ . This is the largest solar flare on record. At around 19:42 UT, intense emission of soft X-rays was detected by *GOES* (*Geostationary Operational Environmental Satellite*) such that the detection was saturated. After 19:42 UT, intense emission of hard X-rays and  $\gamma$ -rays was observed by the *INTEGRAL* spacecraft. Unfortunately, at this time, the *RHESSI* spacecraft was on the night side of the Earth. Figure 7 shows the energy spectrum of  $\gamma$ -rays observed by *INTEGRAL*. In this event, although the components of the line emission produced by de-excited ions, C (4.4 MeV) and O (6.1 MeV), were not prominent, the 2.2 MeV neutron capture line can be clearly seen. Intense bremsstrahlung X-rays and  $\gamma$ -rays were also observed. Figure 8 shows the time profiles of  $\gamma$ -rays for different energy bins that contain line  $\gamma$ -ray components produced as a result of the ion acceleration. There is a delay of the 2.2 MeV neutron capture  $\gamma$ -ray emission from that of the line  $\gamma$ -ray components produced by excited ions of C and O. We can assume that ion acceleration occurred at the same time

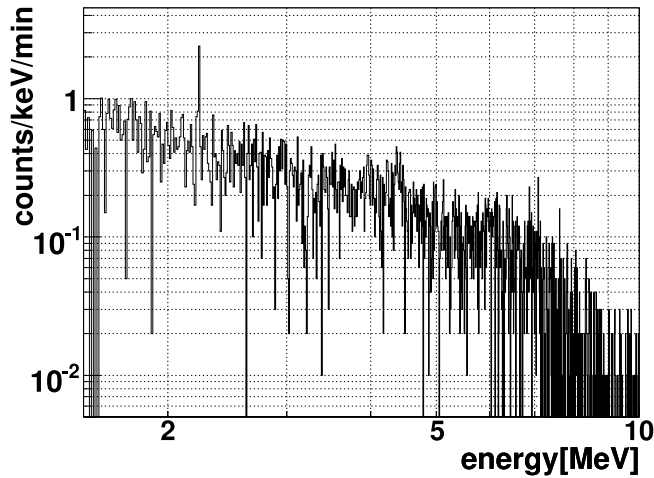


Fig. 7.—Spectrum of  $\gamma$ -rays between 1.5 and 10 MeV observed by *INTEGRAL* from 19:40 to 19:50 UT on 2003 November 4, with background subtracted. A signal produced by 2.2 MeV  $\gamma$ -rays appears superimposed on the bremsstrahlung component. There is weak evidence for 4–7 MeV  $\gamma$ -ray lines.

as the  $\gamma$ -ray lines were emitted, although the main component of these  $\gamma$ -rays is bremsstrahlung. And we can assume that solar neutrons were produced at the same time.

At 19:45 UT, the Sun was located between Hawaii and South America. Although the Chacaltaya observatory was the best place to observe solar neutrons in our international solar neutron telescope network at this time, no data are available because of a data gap. Sierra Negra would also have been a good place to observe solar neutrons, but the Mexico solar neutron telescope had not started continuous observation at that time. Thus, it was necessary to examine data from the Hawaii observatory, which was the third closest of the observatories able to observe solar neutrons.

At 19:45 UT, the zenith angle of the Sun was  $49^{\circ}9'$  at Mauna Kea and  $50^{\circ}5'$  at Haleakala. The air mass along the line of sight to the Sun was 947 and  $1112 \text{ g cm}^{-2}$ , respectively. The other suitable location was Mexico City, where the zenith angle of the Sun was  $40^{\circ}52'$  and the air mass along the line of sight to the Sun was  $1026 \text{ g cm}^{-2}$ . Attenuation of solar neutrons by the Earth's atmosphere above these observatories is calculated using the Shibata model (Shibata 1994). The Haleakala and Mexico City observatories have nearly the same attenuation, while Mauna Kea is located at the best place to observe solar neutrons. However, simultaneous signals were found in both the Haleakala and the Mexico City neutron monitors.

Solar neutrons were observed by the 18NM64 neutron monitor at Haleakala, Hawaii ( $203^{\circ}7\text{E}$ ,  $20^{\circ}7\text{N}$ ; 3030 m a.s.l.). Figure 9 (*top*) shows the 5 minute averages of the counting rate observed on 2003 November 4. At this time, the sampling interval of the Haleakala neutron monitor was 10 s. Clear excesses were seen after 19:45 UT, continuing for 15 minutes. The statistical significances of these excesses are  $4.5 \sigma$  for 19:46:20–19:51:20 UT,  $5.3 \sigma$  for 19:51:20–19:56:20 UT, and  $3.1 \sigma$  for 19:56:20–20:01:20 UT. The total significance for the 15 minutes between 19:46:20 and 20:01:20 UT is  $7.5 \sigma$ . Note that this time interval was just taken to get the maximum significance.

Solar neutrons were also observed by the 6NM64 neutron monitor at Mexico City ( $260^{\circ}8\text{E}$ ,  $19^{\circ}33\text{N}$ ; 2274 m a.s.l.), as shown in Figure 9 (*bottom*). At this time, the sampling interval of the Mexico City neutron monitor was 5 minutes. Clear excesses were seen after 19:45 UT, which was the same time as the excesses observed by the Haleakala neutron monitor. The statistical significances of these excesses are  $2.6 \sigma$  for 19:45–19:50 UT,

$3.1 \sigma$  for 19:50–19:55 UT, and  $3.3 \sigma$  for 19:55–20:00 UT. The total significance for the 15 minutes between 19:45 and 20:00 UT is  $5.2 \sigma$ .

One would expect that Mauna Kea ( $203^{\circ}7\text{E}$ ,  $19^{\circ}8\text{N}$ ; 4200 m a.s.l.) should be a better place to observe neutrons in this event than Haleakala and Mexico City. This is the location of the Hawaii solar neutron telescope with an area of  $8 \text{ m}^2$ , constructed from proportional counters and plastic scintillators, but only a minimal excess was seen after 19:45 UT in the PMT\_L, PMT\_H, and layer1\_with\_anti channels in this telescope as shown in Figure 10. The PMT\_L and PMT\_H are channels of scintillation counter that detect neutrons (recoil protons), the energy thresholds of which are 12 and 20 MeV, respectively. The layer1\_with\_anti is a proportional counter channel, which is located under the scintillation counters. This apparent discrepancy between neutron monitors and the solar neutron telescope is discussed in the next section (§ 3.2.1) considering the surrounding environment of the detector.

### 3.2. Analysis Result

In order to understand the Mauna Kea result, we first use the other observational data to estimate the energy spectrum of the solar neutrons. We begin with the data from the Haleakala monitor because it recorded the largest excess with the best time resolution. We determine the neutron energy by using the TOF method, assuming that all the solar neutrons were produced at 19:45 UT, the peak of the intense emission of high-energy  $\gamma$ -rays observed by *INTEGRAL* as shown in Figure 8. Under this assumption, the energy of neutrons observed by the Haleakala neutron monitor between 19:51:20 and 19:56:20 UT ranged from 59 to 913 MeV.

To derive the energy spectrum of neutrons at the solar surface from the observed time profile by the neutron monitor, the survival probability of neutrons between the Sun and the Earth, the attenuation of solar neutrons passing through the Earth's atmosphere, and the detection efficiency of the neutron monitor must be taken into account. Attenuation is calculated using the Shibata model (Shibata 1994), and we used the detection efficiency calculated by Clem & Dorman (2000).

Using these observational and simulation results, we calculated the energy spectrum of neutrons at the solar surface using the same method as § 2.1. The result is shown in Figure 11. This spectrum was derived from 2 minute averages of the counting rate, where the vertical errors that are shown are only statistical errors. The energy spectrum is well fitted by a power law as

$$Q = (1.5 \pm 0.6) \times 10^{28} \left( \frac{E_n}{100 \text{ MeV}} \right)^{-3.9 \pm 0.5} \text{ MeV}^{-1} \text{ sr}^{-1}. \quad (5)$$

The fitting region is chosen as 100 MeV and above because there the errors from neutron attenuation in the Earth's atmosphere are small. For this fit,  $\chi^2/\text{dof} = 0.92/3 = 0.31$  and the  $\chi^2$  probability is 82%. This spectral index is typical of solar neutron events observed thus far. The total energy flux of neutrons emitted from the Sun in the energy range 59–913 MeV is estimated to be  $3.4 \times 10^{26} \text{ ergs sr}^{-1}$ .

#### 3.2.1. Simulation Using the Impulsive Model

By using the same method of § 2.2.1, time profiles of solar neutrons assuming their spectral index at the solar surface were simulated on the assumption that the neutrons were produced impulsively. We examine the  $\chi^2$  of the fit of the simulated counting rate to the observed excess of the Haleakala neutron monitor obtained from equation (3). In this fitting, data obtained from

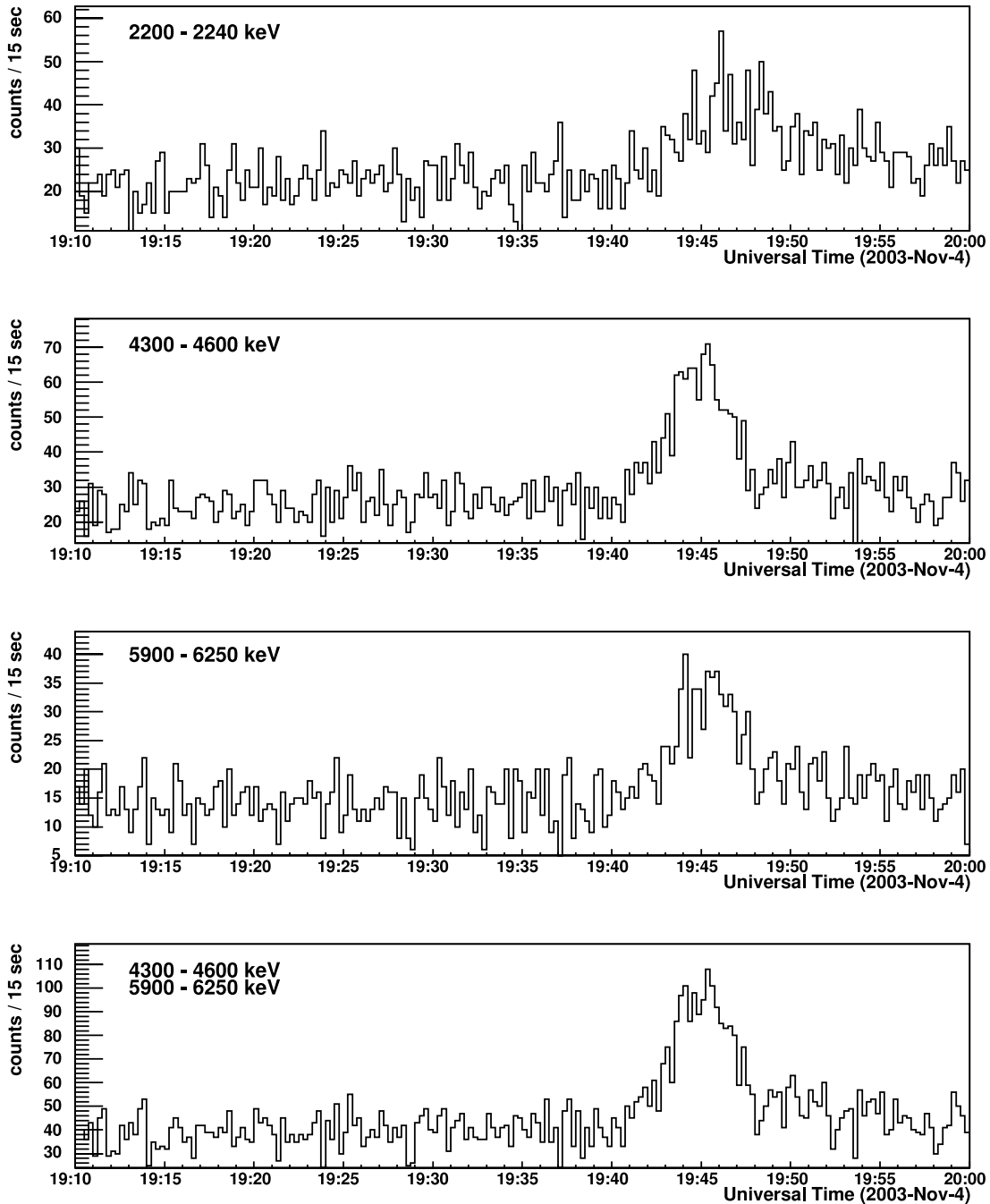


FIG. 8.—Time profiles of  $\gamma$ -ray lines observed by the *INTEGRAL* satellite on 2003 November 4. The bremsstrahlung component has not been subtracted. *Top panel:* Time profile of the 2.2 MeV neutron capture  $\gamma$ -rays. *Second panel:* 4.4 MeV  $\gamma$ -rays of C nuclei. *Third panel:* 6.1 MeV  $\gamma$ -rays of O nuclei. *Bottom panel:* Sum of the data in the second and third panels. Although these time profiles contain line  $\gamma$ -ray components, which indicate the time profile of ion acceleration, the dominant component is bremsstrahlung.

19:45 to 20:06 UT are used. The  $\chi^2$  has its smallest value when the spectral index is around  $-3.9$ . When the spectral index is  $-3.9$ ,  $\chi^2/\text{dof} = 10.3/7 = 1.47$ , which yields the minimum  $\chi^2$  for the simulated time profile (Fig. 12, *top*). From this fitting, the energy spectrum is determined as follows:

$$Q = 2.1_{-0.1}^{+0.2} \times 10^{28} \left( \frac{E_n}{100 \text{ MeV}} \right)^{-3.9_{-0.2}^{+0.1}} \text{ MeV}^{-1} \text{ sr}^{-1}. \quad (6)$$

This is consistent with the result obtained using the simpler method shown in equation (5). The total energy flux of solar neutrons within the energy range 50–1500 MeV is  $6.7_{-0.4}^{+0.5} \times$

$10^{26} \text{ ergs sr}^{-1}$ , about the same order as the calculated value from equation (5).

We have done the same analysis for the Mexico City neutron monitor. In this fitting, data obtained during 19:45–20:05 UT are used. The  $\chi^2$  has its smallest value when the spectral index is around  $-4.3$ . When the spectral index is  $-4.3$ ,  $\chi^2/\text{dof} = 5.55/3 = 1.85$ , which yields the minimum  $\chi^2$  for the simulated time profile (Fig. 12, *bottom*). From this fitting, the energy spectrum is determined as

$$Q = (1.6 \pm 0.2) \times 10^{28} \left( \frac{E_n}{100 \text{ MeV}} \right)^{-4.3 \pm 0.4} \text{ MeV}^{-1} \text{ sr}^{-1}. \quad (7)$$

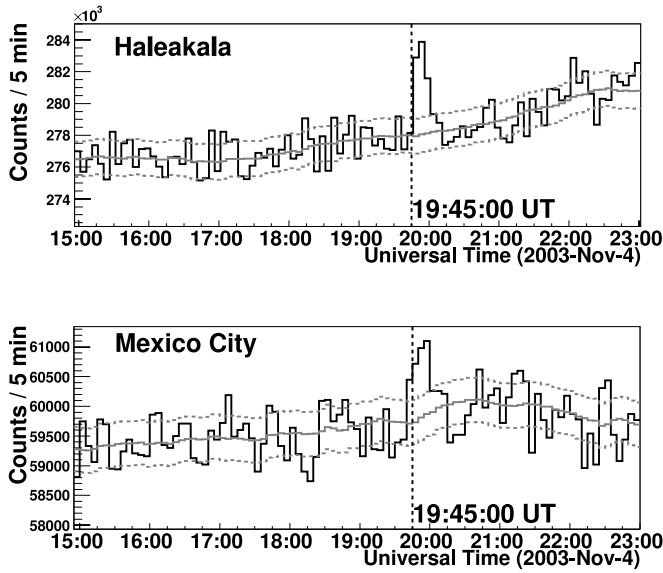


FIG. 9.—Five minute averages of the counting rate observed by the Haleakala (top) and Mexico City (bottom) neutron monitors on 2003 November 4. The smooth solid line is the averaged background, and the dashed lines are  $\pm 1 \sigma$  from the background.

Although the spectral index is softer than the result of the Haleakala neutron monitor, it is consistent with equation (5). The total energy flux of solar neutrons with energies between 50 and 1500 MeV is calculated to be  $(5.4 \pm 0.7) \times 10^{26}$  ergs  $\text{sr}^{-1}$ , about the same order as the result obtained from the analysis of Haleakala.

We then simulated the time profile of neutrons that should be observed from the Hawaii solar neutron telescope using the energy spectrum of incident neutrons obtained from the

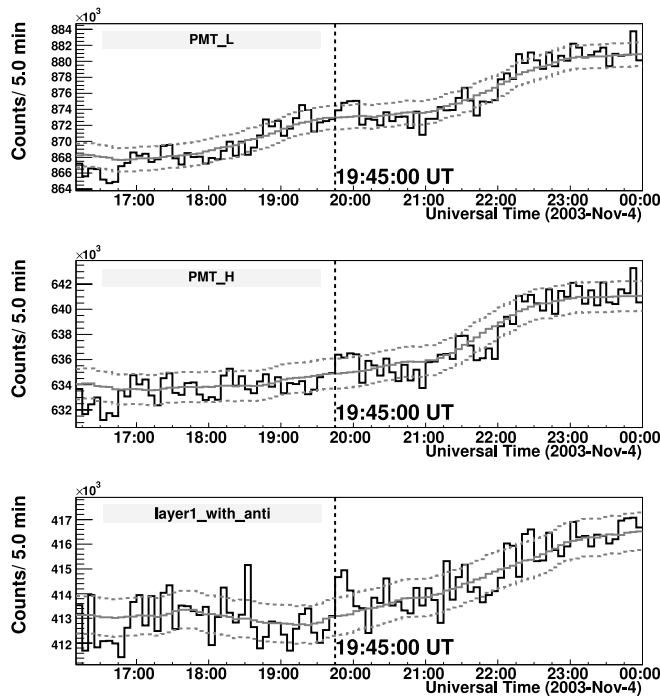


FIG. 10.—Five minute averages of the counting rate of PMT\_L, PMT\_H, and layer1\_with\_anti channels (see details in the text) of the Hawaii solar neutron telescope on 2003 November 4. The solid smooth line is the averaged background, and the dashed lines are  $\pm 1 \sigma$  from the background.

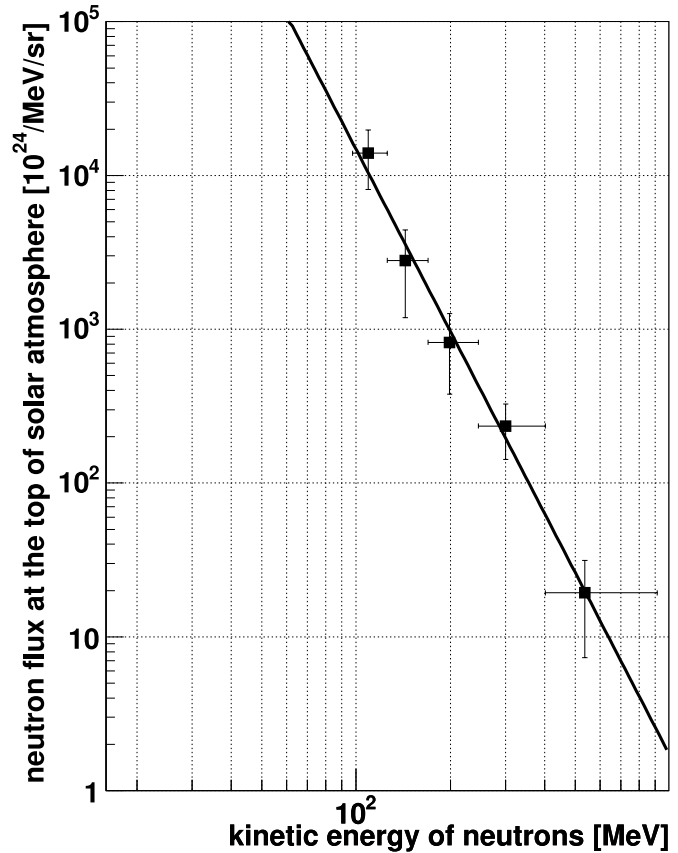


FIG. 11.—Energy spectrum of neutrons at the solar surface on 2003 November 4 calculated from the data of the Haleakala neutron monitor.

data of the Haleakala neutron monitor, namely,  $1.5 \times 10^{28} \times (E_n/100 \text{ MeV})^{-3.9} \text{ MeV}^{-1} \text{ sr}^{-1}$ . We did not attempt to derive a spectrum from the data because excesses of the solar neutron telescope are small.

The detection efficiency of the Hawaii solar neutron telescope is calculated using Geant3, FLUKA-COLOR model. In this calculation,

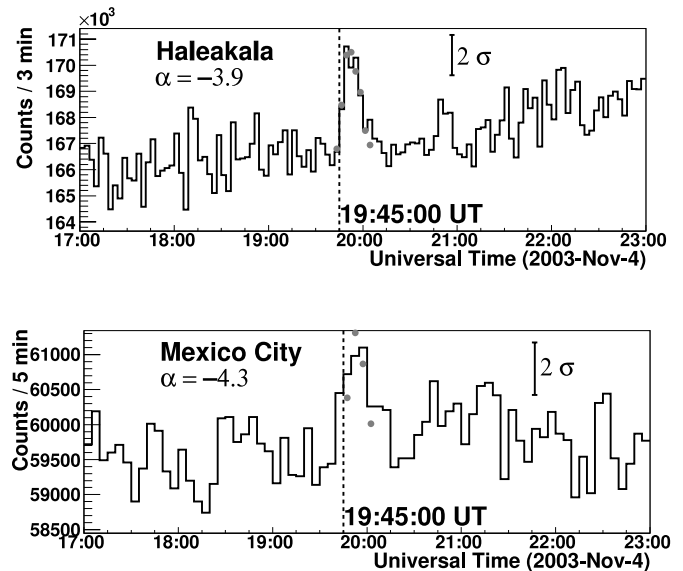


FIG. 12.—Best-fit simulated time profiles (points) when the spectral index is  $-3.9$  for Haleakala (top) and  $-4.3$  for Mexico City (bottom), superposed on the observed counting rate. The start time of the simulated time profile is 19:45 UT, corresponding to the peak time of  $\gamma$ -ray emission.



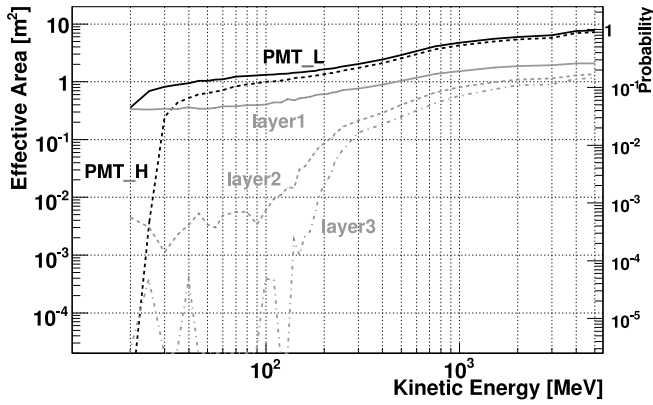


FIG. 13.—Detection efficiencies of the Hawaii solar neutron telescope for neutrons when the detector is surrounded by a 20 cm concrete wall. The black lines indicate the PMT\_L (solid line) and PMT\_H (dashed line) scintillator channels. The gray lines indicate layer channels of layer 1 (solid line), layer 2 (dashed line), and layer 3 (dash-dotted line) with anticoincidence of the anticounter.

the Hawaii solar neutron telescope is surrounded by 20 cm concrete walls, since it is situated within the building housing the SUBARU telescope. Figure 13 shows the detection efficiencies of the Hawaii solar neutron telescope for neutrons and  $\gamma$ -rays.

The simulated result for the layer1\_with\_anti channel of the Hawaii solar neutron telescope, which recorded the largest excess, is shown in Figure 14. For this fitting,  $\chi^2/\text{dof} = 1.24/3 = 0.41$ , so the simulation result is consistent with the observed excess. Because of the high counting rate from the nonhadronic component ( $\gamma$ -ray, muon, and so on) in the Hawaii solar neutron telescope, these excesses are not statistically significant, although they correspond to the same total flux of solar neutrons observed by the Haleakala neutron monitor. It is however possible that solar neutrons actually produced the little hump in the data.

### 3.2.2. Simulation by Neutron Production Using the $\gamma$ -Ray Profile

Next we simulated the neutron time profiles detected at Haleakala and Mexico City by assuming that neutrons were produced with a time spread. The calculation method is the same as in § 2.2.2. For this calculation, we used the  $\gamma$ -ray time profile observed by the *INTEGRAL* satellite during 19:42–19:48:00 UT as the production time profile of solar neutrons, as shown in the bottom panel in Figure 8. The  $\chi^2$  of the fit between observed and simulated time profiles of the Haleakala and Mexico City neutron monitors were calculated. In this fitting, data obtained from

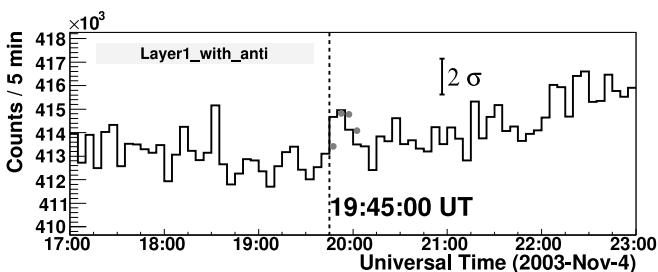


FIG. 14.—Simulated time profile (points) of 5 minute counting rate of layer1\_with\_anti channel of the Hawaii solar neutron telescope on 2003 November 4, superposed on the observational data. The energy spectrum of the incident neutrons is  $1.5 \times 10^{28} (E_n/100 \text{ MeV})^{-3.9} \text{ MeV}^{-1} \text{ sr}^{-1}$ , which was obtained from the data of the Haleakala neutron monitor. The start time of this time profile is 19:45 UT, corresponding to the peak time of  $\gamma$ -ray emission.

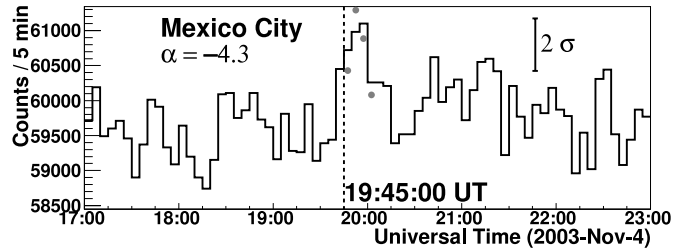
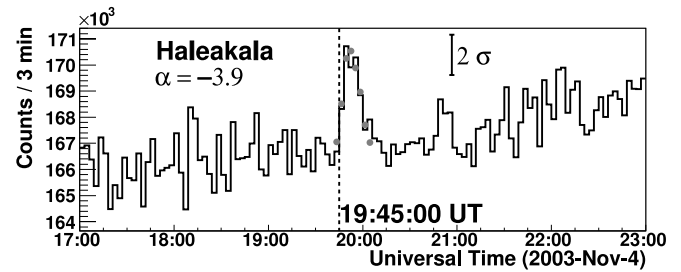


FIG. 15.—Simulated time profiles (points) when the spectral index is  $-3.9$  for Haleakala (top) and  $-4.3$  for Mexico City (bottom), superposed on the observed counting rate of the Haleakala neutron monitor. Points are the simulated time profile for solar neutrons, assuming that they were produced with the same time profile as the high-energy  $\gamma$ -rays shown in Fig. 8.

19:42 to 20:06 UT are used for the Haleakala and from 19:45 to 20:05 UT for the Mexico City neutron monitor. For the Haleakala data, when the power index is  $-3.9$  (Fig. 15, top),  $\chi^2/\text{dof} = 10.57/7 = 1.51$ , giving the minimum value among the simulated time profiles. The spectral index is determined to be  $-3.9 \pm 0.2$ . For the Mexico City data, when the power index is  $-4.3$  (Fig. 15, bottom),  $\chi^2/\text{dof} = 4.28/3 = 1.43$ , giving the minimum value among the simulated time profiles and a spectral index that is determined to be  $-4.3^{+0.4}_{-0.5}$ . The best-fit spectral indices are the same as those derived by assuming that the neutrons were produced impulsively. The total energy fluxes of neutrons are estimated to be  $(7.0 \pm 0.5) \times 10^{26} \text{ ergs sr}^{-1}$  from the Haleakala data and  $5.7^{+0.7}_{-0.8} \times 10^{26} \text{ ergs sr}^{-1}$  from the Mexico City data.

## 4. DISCUSSION AND SUMMARY

Relativistic neutrons were detected in association with the X17.2 solar flare on 2003 October 28 and the X28 solar flare on 2003 November 4. The October 28 event was detected by the Tsubeb neutron monitor, and the November 4 event was detected simultaneously by the neutron monitors at Haleakala and Mexico City and also by the solar neutron telescope at Mauna Kea. During these events, intense emissions of high-energy  $\gamma$ -rays were observed by the *INTEGRAL* satellite.

In order to investigate the production time of solar neutrons, we compared the solar neutron data with the  $\gamma$ -ray data obtained from *INTEGRAL*. In the October 28 event,  $\gamma$ -ray lines from neutron capture and excited ions of C and O nuclei were clearly observed and were quite different from the time profile of bremsstrahlung  $\gamma$ -rays. It appears that the time profile of electron acceleration was distinctly different from the time profile of ion acceleration. From the time profile of neutron capture  $\gamma$ -rays, it seems that high-energy neutrons were produced with the same time profile as  $\gamma$ -ray lines of de-excited ions. In the November 4 event, the time profiles of  $\gamma$ -ray lines, which we have assumed represent the time profile of solar neutron production, cannot be obtained independently, since the bremsstrahlung component was strong and the line  $\gamma$ -ray components were buried in bremsstrahlung. However, from the time profile of the 2.2 MeV neutron

capture  $\gamma$ -rays, it appears that the time profile of ion acceleration was approximately the same as that of bremsstrahlung emissions. Assuming that solar neutrons were produced at the time when these  $\gamma$ -rays were emitted, we could explain the observed excesses.

If we assume that solar neutrons were produced impulsively at 11:05 UT on October 28 and at 19:45 UT on November 4, when the  $\gamma$ -ray lines peak, we can derive the energy spectrum of solar neutrons at the solar surface from the neutron monitors as data by using equations (2) and (5), respectively. For the November 4 event, in order to examine whether all excesses observed by the Haleakala and Mexico City neutron monitors and the solar neutron telescope at Mauna Kea can be expressed by one energy spectrum consistently, and for more detailed analysis, we simulated time profiles of solar neutrons for these detectors and compared with observed time profiles. All of the simulation results are consistent with equation (5) within the range of error as shown in equations (6) and (7). Thus, we could explain all observations with a consistent spectrum.

Although we can fit the data by assuming that solar neutrons are produced impulsively, it is more natural to assume that solar neutrons are produced continuously over a finite time. We therefore modeled the time profiles of solar neutrons by assuming that the neutrons were produced with the same time profile as  $\gamma$ -ray lines from excited ions. For the October 28 event, the spectral indices thus derived are the same as those derived by assuming that neutrons were produced impulsively,  $-3.9$  for Haleakala and  $-4.3$  for Mexico City. In other events, the spectral indices derived by assuming that neutrons are produced continuously tend to be harder than those derived by assuming that neutrons are produced impulsively. However, in this event, since the  $\gamma$ -rays have a symmetric time profile centering around 19:45 UT, there is little difference between the two models. For the November 4 event, the result was that the index obtained using the line  $\gamma$ -ray time profile is clearly harder ( $-2.9$ ) than that

obtained using the impulsive model ( $-3.5$ ). Therefore, for these two events, the observations were explained by assuming that solar neutrons were produced with the same time profile as  $\gamma$ -ray lines.

Although different spectral indices are obtained with a different approach for the October 28 event, these spectral indices are all consistent with the indices calculated from line  $\gamma$ -ray observation by the *RHESSI* satellite (Share et al. 2004) and *INTEGRAL* satellite (Tatischeff et al. 2006).

The spectrum of accelerated ions can be calculated from the neutron spectrum using the spectrum of escaping neutrons produced by the accelerated ions (Hua & Lingenfelter 1987a, 1987b; Hua et al. 2002). From the neutron spectra shown in equations (2) and (5), the number of protons above 30 MeV would be about  $10^{32} \text{ sr}^{-1}$  under the assumption that there is no turnover of the spectrum. This is a typical value for solar neutron events observed thus far.

The authors wish to thank the *INTEGRAL* team for their support to the mission and guidance in the analysis of the *INTEGRAL* satellite data. In particular, we thank A. Bykov and M. Mendez for having kindly permitted us to use their data in advance of publication. We acknowledge the staff member who is managing and maintaining the Tsumeb, Lomnický Stit, Haleakala, and Mexico City neutron monitors. We also thank E. Flüeckiger and R. Bütikofer of the Cosmic Ray Group of the Physikalisches Institut, University of Bern, Switzerland, members of the Armenia group, especially A. A. Chilingarian and N. Gevorgyan, and the staff of the Subaru Telescope for managing and maintaining the Switzerland, Armenia, and Hawaii solar neutron telescopes. We also thank Paul Evenson for reading this manuscript. We wish to thank the referee for evaluating this paper and for helping us to clarify several arguments.

#### REFERENCES

- Bieber, J. W., Clem, J., Evenson, P., Pyle, R., Ruffolo, D., & Sáiz, A. 2005, *Geophys. Res. Lett.*, 32, L03S02
- Chupp, E. L., et al. 1987, *ApJ*, 318, 913
- Clem, J. M., & Dorman, L. I. 2000, *Space Sci. Rev.*, 93, 335
- Debrunner, H., et al. 1997, *ApJ*, 479, 997
- Hua, X.-M., Kozlovsky, B., Lingenfelter, R. E., Ramaty, R., & Stupp, A. 2002, *ApJS*, 140, 563
- Hua, X.-M., & Lingenfelter, R. E. 1987a, *ApJ*, 323, 779
- . 1987b, *Sol. Phys.*, 107, 351
- Lockwood, J. A., & Debrunner, H. 1999, *Space Sci. Rev.*, 88, 483
- Muraki, Y., & Shibata, S. 1996, in *AIP Conf. Proc. 374, High Energy Solar Physics*, ed. R. Ramaty, N. Mandzhavidze, & X.-M. Hua (Woodbury: AIP), 256
- Muraki, Y., et al. 1992, *ApJ*, 400, L75
- Panasyuk, M. I., et al. 2004, *Cosmic Res.*, 42, 489
- Share, G. H., Murphy, R. J., Smith, D. M., Schwartz, R. A., & Lin, R. P. 2004, *ApJ*, 615, L169
- Shea, M. A., Smart, D. F., & Pyle, K. R. 1991, *Geophys. Res. Lett.*, 18, 1655
- Shibata, S. 1994, *J. Geophys. Res.*, 99, 6651
- Shibata, S., Murakami, K., & Muraki, Y. 1993, in *Proc. 23rd Int. Cosmic Ray Conf. (Calgary)*, 3, 95
- Struminsky, A., Matsuoka, M., & Takahashi, K. 1994, *ApJ*, 429, 400
- Tatischeff, V., Kiener, J., & Gros, M. 2006, in *Proc. 5th Rencontres du Vietnam, New Views on the Universe*, in press (astro-ph/0501121)
- Tsuchiya, H., et al. 2001, *Nucl. Instrum. Methods Phys. Res. A*, 463, 183
- Usoskin, I. G., Kovaltsov, G. A., Kananen, H., & Tanskanen, P. 1997, *Ann. Geophys.*, 15, 375
- Valdés-Galicia, J. F., et al. 2004, *Nucl. Instrum. Methods Phys. Res. A*, 535, 656
- Veselovsky, I. S., et al. 2004, *Cosmic Res.*, 42, 435
- Wang, H. T., & Ramaty, R. 1974, *Sol. Phys.*, 36, 129
- Watanabe, K., et al. 2003, *ApJ*, 592, 590